Imaging objects in tissuelike media with optical tagging and the diffuse photon differential transmittance

X. D. Zhu and Sung-po Wei

Department of Physics, University of California, Davis, Davis, California 95616

Xiao Wen Guo

Department of Biological Chemistry, School of Medicine, University of California, Davis, Davis, California 95616

Received December 19, 1995; revised manuscript received July 5, 1996; accepted July 8, 1996

In a proof-of-concept experiment, we optically tagged objects embedded in an inhomogeneous and multiple-scattering medium and measured the difference between the transmitted diffuse photons at two optical wavelengths, one at and the other off a sharp absorption peak of the exogenous contrast agent. We demonstrated that the visibility of tagged objects was significantly enhanced in comparison with that of untagged objects. From our analysis it seems possible to use dual-wavelength differential transmittance spectrometry together with monoclonal-antibody-delivered optical contrast agents to detect tumors as small as 0.1–0.3 cm in size and embedded as deeply as a few centimeters beneath a tissue surface. © 1997 Optical Society of America. [S0740-3232(97)01301-X]

1. INTRODUCTION

In recent years the propagation and distribution of diffuse photons in highly scattering media have attracted considerable attention in the field of medical imaging.[1–19] This interest is motivated by the fact that near-infrared electromagnetic waves from 730 to 900 nm are strongly scattered and yet only weakly absorbed in human tissues such as skin and breast.[7] Since light is multiply scattered, its propagation characteristics can be described by a diffusion approximation.[20,21] The latter is perturbed by inhomogeneities with differing optical properties, such as tumor growths in an otherwise normal tissue. By measuring the transmitted or the reflected diffuse photons, one may deduce information about the locations and sizes of these inhomogeneities with sufficient certainty. Even though the extraction of imaging information from diffuse light is complicated and less straightforward in comparison with the x-ray-attenuation-based imaging techniques, the research efforts of many groups have continued to be fueled by the possibility that the near-infrared optical imaging technique in some form may eventually become a noninvasive alternative to x-ray mammography for early detection of cancerous growths.[1–19,22,23]

In the past decade diffuse photon spectrometry in the form of transillumination light-scanning spectroscopy has been explored and tested in the field of medical imaging.[1–6] By detecting the transmittance of diffuse light at red and near-infrared wavelengths with an eight-bit video imaging camera, one obtains either a differential transmittance or a relative transmittance. The identification of cancerous growth was based on empirical observations that malignant tumors, accompanied by higher densities of blood vessels, cause either an enhanced regional or a total absorption in one breast while not in the other, or they cause a relative enhanced absorption of the near-infrared light. In a series of clinical tests in the 1980's, however, the transillumination light-scanning technique was shown to be inferior to x-ray mammography because of its lack of specificity and its inadequate sensitivity to nonpalpable tumors of sizes less than 1 cm and to even larger tumors that are embedded a few centimeters beneath the skin surface.[3–5] It is recognized that with improved understanding of light propagation in highly scattering media and the advancement of the detection and biotechnology, one should be able to improve the sensitivity, specificity, and spatial resolution of light-scan transillumination.[6] At the present time, diffuse photon or transillumination imaging for cancer detection remains experimental.

Significant progress has been made recently as a result of strong research efforts in both condensed matter physics and medical imaging communities to better understand light propagation in multiple-scattering media.[6,7,11–19,20] For example, it is well known now that modulating the amplitude of an illuminating light source causes the alternating portion of the diffuse photon density to behave much like a damped wave that interferes and diffracts.[11–14] By exploiting the interference effect, many groups have been able to improve the spatial resolution of diffuse photon imaging to a fraction of a millimeter.[11–14,17] The high accuracy in locating objects in multiple-scattering media has benefited from a more quantitative understanding of diffuse photon propagation.[15–19] It is also recognized that the use of optical contrast agents in transillumination imaging improves the sensitivity.[1,12] The same concept has already been used in magnetic resonance imaging. In the studies performed so far, optical contrast agents were explored

0740-3232/97/010300-06$10.00

mainly as a means to enhance the overall absorption of an optically tagged tissue in the near-infrared region from 730 to 900 nm. On the technology side, it has recently become feasible to deliver large enough amounts of contrast agents with monoclonal antibodies to specific tumors.[24] However, one crucial question remains as to whether diffuse photon imaging with the current use of optical contrast agents would have a sufficient specificity in detecting tumors in a human breast, where there exist normal inhomogeneities such as macro cysts. This is the subject of this paper.

We intend to show another aspect of optical contrast agents that can be exploited in diffuse photon imaging to dramatically enhance the visibility of a tumor in the presence of other lumpy structures that are present even in a normal human breast. Our approach is to exploit the sharpness of the absorption peak of an optical contrast agent, not just the enhanced optical absorption. This form of dual-wavelength differential measurement enables us to distinguish with significantly improved contrast optically tagged objects from untagged lumpy structures. As far as we know, this aspect has not been explored by others. To prove the concept, we conduct a continuous-wave or d.c. transillumination imaging experiment in which we selectively tag objects embedded in a tissue phantom with an optical contrast agent. We then measure the difference in the transmittance at two optical wavelengths, one at an absorption maximum of the agent and the other off the maximum on the steep side of the absorption peak. We find that the visibility of the tagged objects is significantly enhanced in comparison with that of the untagged objects. Our preliminary results further show that by using 16-bit rather than 8-bit CCD detectors, we can improve the sensitivity of tumor detection such that it seems feasible to detect optically tagged tumors as small as 0.1–0.3 cm in size and embedded as deep as a few centimeters beneath the skin surface of human tissue.

2. SAMPLE PREPARATION AND EXPERIMENTAL PROCEDURES

A sketch of the experimental setup is shown in Fig. 1. We use suspended TiO_2 powder (supplied by Sigma Coatings) in glycerin at a concentration of 0.7% by volume and an Intralipid emulsion at a concentration of 20% by weight (from Kabi Pharmacia, Clayton, N.C.) as tissue phantoms. They are contained in a 5-mm $\times$ 50-mm $\times$ 50-mm glass cell. For objects or inhomogeneities, we use glass capillary tubes and 0.3-mm Pentel carbon filament. The capillary tubes have inner diameter (i.d.) of 0.3 mm and outer diameter (o.d.) of 1.2 mm and can be filled with optical contrast agents. For the latter, we use solutions of dichlorotriazinylaminofluorescein (DTAF) in dimethyl sulfoxide (DMSO) (from Calbiochem, La Jolla, Calif., $\lambda_{max} = 492$ nm, $\epsilon_{max} = 82$ cm^{-1} mM^{-1}, M.W. = 531.7). From the measurements of Blakeslee and Baines, we know that the extinction coefficient ϵ at 488.0 nm is close to 80% of the maximum, drops to 20% of the maximum at 514.5 nm, and is essentially zero at 632.8 nm.[25] We thus choose two of the emission lines of an Argon-ion laser, one at 488.0 nm and the other at 514.5 nm, and a He–Ne laser at 632.8 nm as illuminating light sources. We measured the light-scattering mean free paths in the two tissue phantoms using the same method as described in Ref. 26. In the TiO_2 suspension, the values at all three wavelengths are essentially the same, $l_{sc} = 15.0\ \mu m \pm 0.3\ \mu m$. In the Intralipid emulsion, the scattering mean free paths are more dispersive, with $l_{sc} = 8.60 \pm 0.02\ \mu m$ at 488.0 nm, $l_{sc} = 9.77 \pm 0.02\ \mu m$ at 514.5 nm, and $l_{sc} = 16.15 \pm 0.06\ \mu m$ at 632.8 nm. Our measurement compares well with that of van Staveren and co-workers; in particular, our result reproduces the wavelength dependence of $l_{sc} \propto \lambda^{2.4}$ reported by these authors.[27] The optical path length of the cell ($L = 5$ mm) thus covers 300–500 scattering mean free paths.

We expand the laser beam with a combination of lenses such that one of the 50-mm $\times$ 50-mm cell surfaces is uniformly illuminated. We measure the near-field distribution of the transmitted light from the opposite surface. This is done by imaging an area of 46 mm $\times$ 46 mm on the opposite (back) surface at a 4-to-1 reduction ratio onto the detection surface of either a CCD camera or a scanning photodiode. The solid angle of collection is 3×10^{-3} steradians, so we can neglect the influence of the glass–air interface on the intensity distribution. The CCD camera is a 16-bit TK512CB/AR (Photometrics, Tucson, Ariz.). The photodiode is a EG&G FND100 (EG&G Photon Devices, Sunnyvale, Calif.). With the photodiode we modulate the amplitude of the illuminating light sources at a low frequency of 1000 Hz and detect the a.c. component of the photocurrent with a lock-in amplifier. With the CCD camera, we use the unmodulated illuminating sources and detect the total photon counts. We typically accumulate 5×10^5 photon counts in each pixel.

In all the measurements we first record the near-field distribution of the transmitted diffuse photons with only the tissue phantom; we then insert objects into the cell and repeat the measurement again. We take the ratio of the two data sets as the normalized transmittance. When the CCD detector is used, we also take care to subtract the dark counts accumulated over the same exposure time period from the two data sets before taking the ratio.

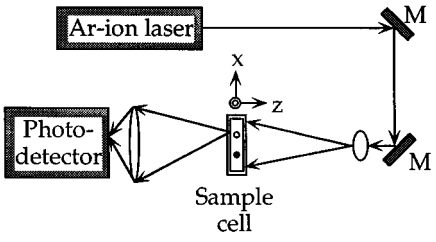

Fig. 1. Sketch of the experimental setup for measurements of the near-field transmittance of diffuse photons through a cell containing a multiple-scattering medium. M's reflection mirrors. The open circle represents the top view of an empty capillary tube, and the filled circle represents a solution-filled capillary tube. They are used as untagged and tagged objects, respectively, for imaging. The sample cell contains a homogeneous multiple-scattering medium as the tissue phantom.

3. EXPERIMENTAL RESULTS

To demonstrate the sharp wavelength dependence of the near-field transmittance as a result of optical tagging of an embedded object, we use a capillary tube filled with a DTAF solution at a concentration of 7.6×10^{-2} molar (M). The tube is placed (along the y axis) in the middle of the cell, parallel to both the front (the illuminated) and the back surface. In this measurement the TiO_2 suspension (in glycerin) is used as the tissue phantom, and the photodiode is used to scan horizontally across the image plane (along the x axis). Hence the object is at a position 160 scattering mean paths from both surfaces of the tissue phantom. The measurement is performed at each of the three optical wavelengths; the results are displayed in Fig. 2. The near-field transmittance dips at the lateral position (the x coordinate) where the tube is placed. This feature reproduces the observation made by den Ouder and co-workers.[17] The most important feature here is the sharp wavelength dependence. The magnitude of the dip decreases as the wavelength increases from 488.0 to 632.8 nm. In fact, at $\lambda = 632.8$ nm, where DTAF is no longer absorbant, the dip disappears and the near-field transmittance bears a weak feature that is typical of a nonabsorbing object in a highly scattering medium.[17]

The difference between any two of the three curves in Fig. 2 may serve as an example of the enhancement of the object visibility in a dual-wavelength differential transmittance. To demonstrate this aspect more directly, we show in Fig. 3 the near-field transmittance at 514.5 and 488.0 nm with three objects in the cell. One object is an empty capillary tube. The second one is a capillary tube that contains the DTAF solution (7.6×10^{-2} M). The third object is a 0.3-mm-diameter Pentel carbon filament as a perfect absorber. Also shown in Fig. 3 is the difference between the transmittance at 514.5 nm and the one at 488.0 nm, which we call the differential transmittance. The visibility of the tube containing DTAF is clearly enhanced as the visibility of the spectrally flat empty tube and carbon filament are suppressed in the differential transmittance. The signal-to-noise ratios displayed in Figs. 2 and 3 are limited by the total data acquisition time. The latter is limited to a few minutes by the downward drift of TiO_2 powder toward the cell bottom. Over the few minutes' time, we had to perform measurements at 200 sampling positions.

To show that the signal-to-noise ratio can be improved with a stable tissue phantom and to assess properly the sensitivity of the dual-wavelength differential transmittance to small objects, we performed a series of measurements with the Intralipid emulsion as the tissue phantom.[27] The latter is stable in the air for tens of hours. Furthermore, we use a 16-bit CCD camera (Photometrics TK512CB/AR) as a photodetector so that we can simultaneously record the near-field transmittance at all sampling positions on the image plane. Assuming that the noise is limited by the photon statistics, this enables us to achieve the highest signal-to-noise ratio for a fixed data acquisition time. In the results shown below, we accumulate roughly 5×10^5 photon counts in each pixel before normalization. In Figs. 4(a) and 4(b) we display the near-field transmittance over an area 3.2×1.3 mm on the back surface of the cell. We have as objects an empty capillary tube and a tube filled with a DTAF solution at 3.8×10^{-2} M. These objects are roughly in the middle of the tissue phantom. In Fig. 4(c) we display the differential transmittance. We note again that the visibility of the tube with the DTAF solution is preferentially enhanced. Furthermore, the signal-to-noise ratio is also greatly improved. In fact, the peak-to-peak noise is roughly 0.2–0.3% in the differential transmittance, which is predominantly statistical, associated with 5×10^5 photon counts per pixel. The residual signal from the empty tube is the result of the difference in the scattering mean free paths at 514.5 and 488.0 nm.

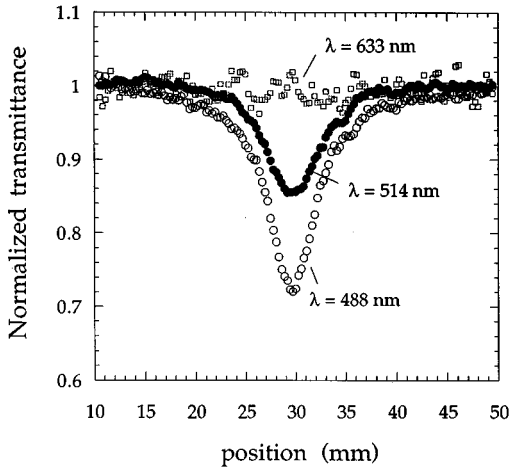

Fig. 2. Normalized near-field transmittance of diffuse photons at three wavelengths. The sample cell is filled with a TiO_2 suspension (in glycerin) at a volume concentration of 0.7%. In the middle of the cell is a 0.3-mm-i.d. capillary tube filled with a DTAF solution (in DMSO) at a concentration of 7.6×10^{-2} M.

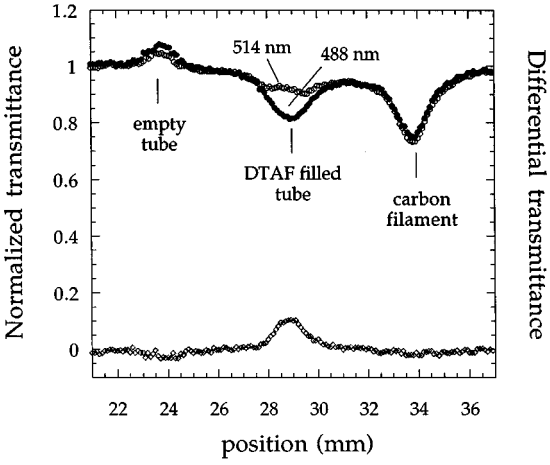

Fig. 3. Normalized near-field transmittance at 514 and 488 nm. The sample cell is filled with a TiO_2 suspension (in glycerin) at a volume concentration of 0.7%. In the middle are an empty 0.3-mm-i.d. capillary tube, a 0.3-mm capillary tube filled with a DTAF solution (in DMSO) at 7.6×10^{-2} M, and a 0.3-mm-diameter Pentel carbon filament. Also displayed is the difference between the transmittance at 514 nm and the one at 488 nm.

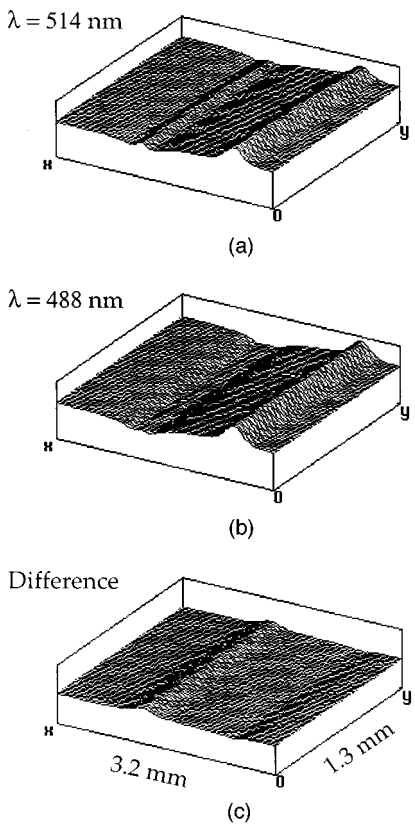

Fig. 4. (a) Normalized near-field transmittance at 514 nm over an area 3.2 mm × 1.3 mm on the exit surface. The sample cell is filled with a 20% Intralipid emulsion (see text). It also contains two capillary tubes. On the far left is the feature caused by the tube filled with a DTAF solution (in DMSO) at 3.8×10^{-2} M; on the right is the feature caused by the empty tube. (b) Normalized near-field transmittance at 488 nm over the same area under the same condition. (c) The difference between the transmittance at 514 nm and the one at 488 nm. The visibility of the tube with the DTAF solution is clearly enhanced in the differential transmittance.

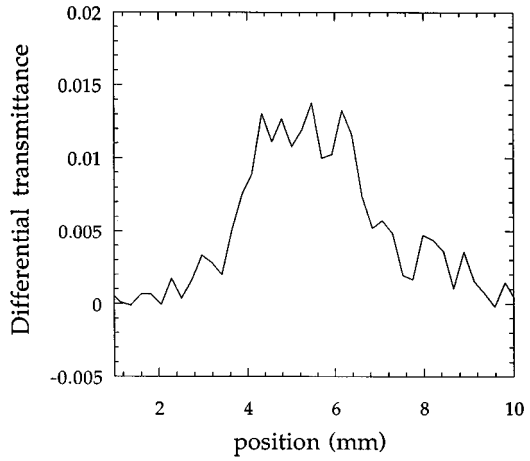

Fig. 5. Near-field differential transmittance between the transmittance at 514 nm and that at 488 nm. The sample cell is filled with a 20% Intralipid emulsion. In the middle of the cell is a 0.3-mm-i.d. capillary tube containing a 0.5-mm-long segment of DTAF solution (in DMSO) at 3.8×10^{-2} M.

To quantify the sensitivity of the differential transmittance to a minute amount of optical contrast agents localized in a tissue phantom, we use a capillary tube that holds a small segment of DTAF solution. The dimension of the segment is 0.5 mm in length and 0.3 mm in diameter. At the concentration of 3.8×10^{-2} M the segment contains 1.3×10^{-9} moles of DTAF. The tube is placed in the middle of the cell or 250 scattering mean free paths from both the front and the back surfaces of the tissue phantom. In Fig. 5 we display a line scan of the differential transmittance along the axis of the segment. The peak of the differential transmittance is 0.013, or 1.3% of the total normalized transmittance. For a small solution segment the spatial distribution of the differential transmittance far from the segment is independent of the segment shape, so the peak change measures the total amount of the contrast agents. The noise of 0.3% is again limited predominantly by photon statistics.

4. DISCUSSION

From the experimental results presented in Section 3, it is clear that using optical contrast agents in a dual-wavelength differential transmittance measurement with the two wavelengths near a sharp absorption peak of the agent dramatically improves the visibility of the optically tagged objects. We emphasize here that simply tagging the objects of interest without exploiting the sharp absorption feature of the contrast agent is not sufficient for identifying the tagged objects in the presence of other untagged and yet more massive inhomogeneities. Consequently, our approach clearly enhances the specificity of transillumination imaging, provided that the optical contrast agents can be delivered with specificity through, for example, monoclonal antibodies. Such monoclonal antibodies in fact exist and have been used to deliver contrast agents suitable for magnetic resonance imaging of breast cancer.[28]

It is also clear that the use of a 16-bit CCD camera improves the signal-to-noise ratio and in turn the sensitivity of transillumination imaging when the noise is limited by photon statistics (as is the case in our investigation). The improvement of the sensitivity with the use of a 16-bit CCD camera over that with an 8-bit CCD camera can be understood as follows. For scientific CCD cameras the achievable detection limit is limited by the readout noise, which is typically one analog-to-digital conversion unit. For a 16-bit camera this corresponds to one part in 65,000, or 0.0015%. For an 8-bit camera it is one part in 256, or 0.4%. If we require a detection signal-to-noise ratio of 4, the minimum detectable differential transmittance will be 1.6% for an 8-bit camera and 0.006% for a 16-bit camera. Therefore by using 16-bit or even 18-bit cameras as photodetectors, we should be able to improve the sensitivity of transillumination imaging by two to three orders of magnitude from what was achievable in the previous transillumination light-scanning studies.[1–5,29,30]

There remain a number of practical issues that should be addressed if the present improvement is to lead to a viable optical method for early detection of small cancerous growths in human breasts. The first is whether the

absolute sensitivity of the present differential transmittance technique is adequate under realistic conditions of tissues and deliverable concentrations of optical contrast agents. Since the noise in our measurement is limited by photon statistics, it can be reduced further by a factor of 50 by simply increasing the photon counts. In that case we should be able to detect 25 picomoles of DTAF (with the same signal-to-noise ratio of 4) on a tagged object at a distance of 250 scattering mean free paths from a tissue surface. Since the average thickness of a compressed human breast is 4.2 cm and the scattering mean free path in the near-infrared transparency window of a human breast is 0.06 cm,[7] the middle of a compressed human breast is only 35 scattering mean free paths from the skin surface. This means that we should be able to detect a tumor in the middle of a human breast carrying only 4 picomoles of optical contrast agents such as DTAF.[15,17] Moreover, the detection limit can be further reduced to less than 2 picomoles if indocyanine green (ICG) (λ_{max} = 805 nm, $\epsilon_{max} = 200\ cm^{-1}\,mM^{-1}$, M.W. = 770) is used as a contrast agent. ICG is 2.5 times as absorptive in the near-infrared as DTAF in the visible range.[7] For a tumor 0.1 cm in diameter, this translates to a concentration of 1–2 nanomoles or 2–3 μg of indocyanine green per gram of tumor, or 2×10^{-3} mM. At this level of optical tagging, the absorption coefficient of the tagged tumor at λ_{max} = 805 nm is $\mu_a = 0.4\ cm^{-1}$, which is ten times as large as the averaged absorption coefficient of a normal human breast. Such a concentration is far below the safe level of 50 μg per gram of tumor approved by the U.S. Food and Drug Administration. The question then becomes whether such a concentration of indocyanine green can be delivered to a designated tumor. In nuclear medicine, monoclonal antibodies are often used to deliver radioactive labeling or heavy elements to specific tissues such as malignant tumors for radioimmunodiagnosis or radioimmunotherapy. It is common that a concentration of 50 picomoles or more of antibodies per gram of tumor is delivered. Usually, 10–20 radioactive labelings can be carried by one antibody with current signal amplification schemes.[31] Consequently, it should be fairly easy to deliver 0.5–2 nanomoles of optical contrast agent such as indocyanine green. This is already adequate for our proposed goal to detect 0.1 cm tagged tumor with a photon statistics-limited signal-to-noise ratio better than 4. Recently Kassis and co-workers have demonstrated that the number of labelings per monoclonal antibody can be enhanced even further.[24] If the targeted-signal augmentation reaches 200–500, we expect to be able to deliver a dosage of 10–25 nanomoles of indocyanine green per gram of tumor.[32] At such a dosage level we should be able to detect tumors 0.1 cm in size and embedded a few centimeters beneath the skin surface with a signal-to-noise ratio much better than 4.

In the present study, we use the empty glass tube and the Pentel filament to simulate inhomogeneities that are not tagged by optical contrast agents. In reality, the inhomogeneous structures, including blood vessels that already exist in a normal human breast, do not have as flat an optical response as our phantom objects. In addition, the absorption of a normal tissue should also vary to some degree with the optical wavelength within the near-infrared window.[7] It is possible to find a region in the near-infrared spectral window where the absorption of the tissue varies little with the wavelength. The dual-wavelength transmittance is preferably carried out in this region. We need more spectroscopic information to further quantify and model the residual contributions from the normally present lumpy structures in a breast. Empirically, the differential transmittance from these structures can be measured in the absence of optical contrast agents. Once their contributions are characterized, they can be subtracted from the transmittance obtained after the optical contrast agents are delivered. The effectiveness of such an empirical approach remains to be further explored and optimized.

5. CONCLUSION

We reiterate that the dual-wavelength differential transmittance measurement of multiply scattered light makes possible the detection of optically tagged objects with significantly enhanced visibility. Our analysis further demonstrates the feasibility of detecting tumors as small as 0.1 cm in diameter and embedded as deeply as a few centimeters beneath a tissue surface. Although many technical issues remain to be worked out, such an effort seems very worthwhile. Considering that the early d.c. transillumination light-scanning technique already has had reasonable success in detecting breast cancers larger than 1 cm in diameter, it is more than simply optimistic to believe that with the currently prescribed object visibility enhancement in combination with the use of high-resolution CCD detectors and the interference effect of diffuse photon density waves (a.c. transillumination), one should be able to detect deeply embedded tumors with diameters far less than 1 cm with adequate sensitivity, spatial resolution, and specificity.

ACKNOWLEDGMENT

The authors thank Photometrics for the loan of the CCD camera used in this work.

Address correspondence to X. D. Zhu at the address on the title page or tel: 916-752-4689; fax: 916-752-4717; e-mail: xdzhu@ucdphy.ucdavis.edu.

REFERENCES

1. M. Cutler, "Transillumination of the breast," Surg. Gynecol. Obstet. **48**, 721–727 (1929); C. J. D'Orsi, R. J. Bartrum, and M. M. Moskowitz, "Lightscanning of the breast," in *Breast Cancer Detection: Mammography and Other Methods in Breast Imaging*, Lawrence W. Bassett and Richard H. Gold eds., 2nd ed. (Grune & Stratton, Orlando, Fla., 1987), pp. 169–177.
2. R. Morton and S. S. Miller, "Infrared transillumination using photography and television (videodioscopy)," J. Audiovisual Media Med. **4**, 86–90 (1981); D. J. Watmough, "Transillumination of breast tissues: factors governing optimal imaging of lesions," Radiology **147**, 89–92 (1982).
3. R. J. Bartrum and H. C. Crow, "Transillumination light-scanning to diagnose breast cancer: a feasibility study," Am. J. Roentgenology **142**, 409–414 (1984); E. A. Sickles, "Breast cancer detection with transillumination and mammography," Am. J. Roentgenology **142**, 841–844 (1984);

G. E. Geslien, J. R. Fisher, and C. DeLaney, "Transillumination in breast cancer detection: screening failure and potential," Am. J. Roentgenology **144**, 619–622 (1985); J. J. Gisvold, L. R. Brown, R. G. Swee, D. J. Raygor, N. Dickerson, and M. K. Ranfranz, "Comparison of mammography and transillumination light scanning in the detection of breast cancer," Am. J. Roentgenology **147**, 191–194 (1986).
4. E. A. Sickles, "Imaging techniques other than mammography for the detection and diagnosis of breast cancer," in *Recent Results in Cancer Research*, S. Brünner and B. Langfeldt, eds. (Springer-Verlag, New York, 1990), Vol. 119, pp. 127–135.
5. H. Key, P. C. Jackson, and P. N. T. Wells, "New approaches to transillumination imaging," J. Biomed. Eng. **10**, 113–118 (1988).
6. S. Fantini, M. Franceschini, G. Gaida, E. Gratton, H. Jess, W. W. Mantulin, K. T. Moesta, P. Schlag, and M. Kaschke, "Frequency-domain optical mammography: edge effect corrections," Med. Phys. **23**, 149–157 (1996), and references therein.
7. A. Yodh and B. Chance, "Spectroscopy and imaging with diffusing light," Phys. Today **48**, 34–40 (1995); W. F. Cheong, S. A. Prahl, and A. J. Welch, "A review of the optical properties of biological tissues," IEEE J. Quantum Electron. **26**, 2166–2185 (1990).
8. *Photon Migration and Imaging in Random Media and Tissues*, B. Chance and R. R. Alfano, eds., Proc. SPIE **1888** (1993).
9. R. R. Alfano, ed., *Advances in Optical Imaging and Photon Migration*, Vol. 21 of OSA Proceedings Series (Optical Society of America, Washington, D.C., 1994).
10. B. Chance and R. R. Alfano, eds., *Optical Tomography, Photon Migration, and Spectroscopy of Tissue and Model Media: Theory, Human Studies, and Instrumentation*, Proc. SPIE **2389** (1995).
11. J. M. Schmitt, A. Knüttel, and J. R. Knutson, "Interference of diffusive light waves," J. Opt. Soc. Am. A **9**, 1832–1843 (1992); A. Knüttel, J. M. Schmitt, and J. R. Knutson, "Spatial localization of absorbing bodies by interfering diffusive photon-density waves," Appl. Opt. **32**, 381–389 (1993); A. Knüttel, J. M. Schmitt, R. Barnes, and J. R. Knutson, "Acoustic-optic scanning and interfering photon density waves for precise localization of an absorbing (or fluorescent) body in a turbid medium," Rev. Sci. Instrum. **64**, 638–644 (1993).
12. B. Chance, K. Kang, L. He, J. Weng, and E. Sevick, "Highly sensitive object location in tissue models with linear in-phase and anti-phase multi-element optical arrays in one and two dimensions," Proc. Natl. Acad. Sci. USA **90**, 3423–3427 (1993).
13. M. A. O'Leary, D. A. Boas, B. Chance, and A. G. Yodh, "Experimental images of heterogeneous turbid media by frequency-domain diffuse-photon tomography," Opt. Lett. **20**, 426–428 (1995).
14. D. A. Boas, M. A. O'Leary, B. Chance, and A. G. Yodh, "Scattering and wavelength transduction of diffuse photon density waves," Phys. Rev. E **47**, R2999–3002 (1993).
15. D. A. Boas, M. A. O'Leary, B. Chance, and A. G. Yodh, "Scattering of diffuse photon density waves by spherical inhomogeneities within turbid media: analytic solution and applications," Proc. Natl. Acad. Sci. USA **91**, 4887–4891 (1994).
16. R. Berkovits and Shechao Feng, "Theory of speckle-pattern tomography in multiple-scattering media," Phys. Rev. Lett. **65**, 3120–3123 (1990).
17. P. N. den Outer, Th. M. Nieuwenhuizen, and A. Lagendijk, "Location of objects in multiple-scattering media," J. Opt. Soc. Am. **10**, 1209–1218 (1993); Th. M. Nieuwenhuizen and M. C. W. van Rossum, "Role of a single scatterer in a multiple scattering medium," Phys. Lett. A **177**, 102–106 (1993).
18. Shechao Feng, Fan-An Zeng, and B. Chance, "Photon migration in the presence of a single defect—a perturbation analysis," Appl. Opt. **34**, 3826–3837 (1995).
19. S. Feng, F. Zeng, and B. Chance, "Monte Carlo simulations of photon migration path distribution in multiple scattering media," in *Photon Migration and Imaging in Random Media and Tissues*, B. Chance and R. R. Alfano, eds., Proc. SPIE **1888**, 78–89 (1993).
20. A. Ishimaru, *Wave Propagation and Scattering in Random Media* (Academic, New York, 1978).
21. H. C. van de Hulst, *Multiple Light Scattering* (Academic, New York, 1980), Vols. I and II.
22. *Breast Cancer Detection: Mammography and Other Methods in Breast Imaging*, Lawrence W. Bassett and Richard H. Gold, eds., 2nd ed. (Grune & Stratton, Orlando, Fla., 1987).
23. R. H. Gold, *Breast Cancer Detection through Mammography* (Medcom, New York, 1976).
24. A. I. Kassis, P. L. Jones, K. Z. Matalka, and S. J. Adelstein, "Antibody-dependent signal amplification in tumor xenografts after pretreatment with biotinylated monoclonal antibody and avidin or streptavidin," J. Nucl. Med. **37**, 343–352 (1995).
25. D. Blakeslee and M. G. Baines, "Immunofluorescence using dichlorotriazinylaminofluorescein (DTAF). I. Preparation and fractionation of labeled IgG," J. Immunol. Methods **13**, 305–320 (1976).
26. M. B. van der Mark, M. P. van Albada, and A. Lagendijk, "Light scattering in strong scattering media: multiple scattering and weak localization," Phys. Rev. B **37**, 3575–3592 (1988).
27. H. J. van Staveren, C. J. M. Moes, J. van Marle, S. A. Prahl, and M. J. C. van Gemert, "Light scattering in Intralipid-10% in the wavelength range of 400–1100 nm," Appl. Opt. **30**, 4507–4514 (1991); S. T. Flock, S. L. Jacques, B. C. Wilson, W. M. Star, and M. J. van Gemert, "Optical properties of Intralipid: a phantom medium for light propagation studies," Lasers Surg. Med. **12**, 510–519 (1992).
28. K. Orang-Khadivi, B. L. Pierce, C. M. Ollom, L. Jean Floyd, R. L. Siegle, and R. F. Williams, "New magnetic resonance imaging techniques for the detection of breast cancer," Breast Cancer Res. Treat. **32**, 119–135 (1994).
29. J. R. Singer, F. A. Grunbaum, P. Kohn, and J. P. Zubelli, "Imaging reconstruction of the interior of bodies that diffuse radiation," Science **48**, 990–993 (1990).
30. H. Jiang, Y. Qian, and K. T. Rhee, "High-speed dual-spectra infrared imaging," Opt. Eng. **32**, 1281–1289 (1992).
31. Sui Shen and G. DeNardo, School of Medicine, University of California, Davis, Davis, Calif. 95616 (personal communication, August 1995).
32. The feasibility of a target-signal augmentation up to 200–1000 was communicated to the authors by A. I. Kassis, Harvard Medical School, Boston, Mass. (personal communication, October 1995).